

Electronic Supplementary Material

Crown ether-thiourea conjugates as ion transporters

Zhixing Zhao¹, Bailing Tang¹, Xiaosheng Yan (✉)¹, Xin Wu (✉)², Zhao Li¹, Philip A. Gale (✉)^{2,3}, Yun-Bao Jiang (✉)¹

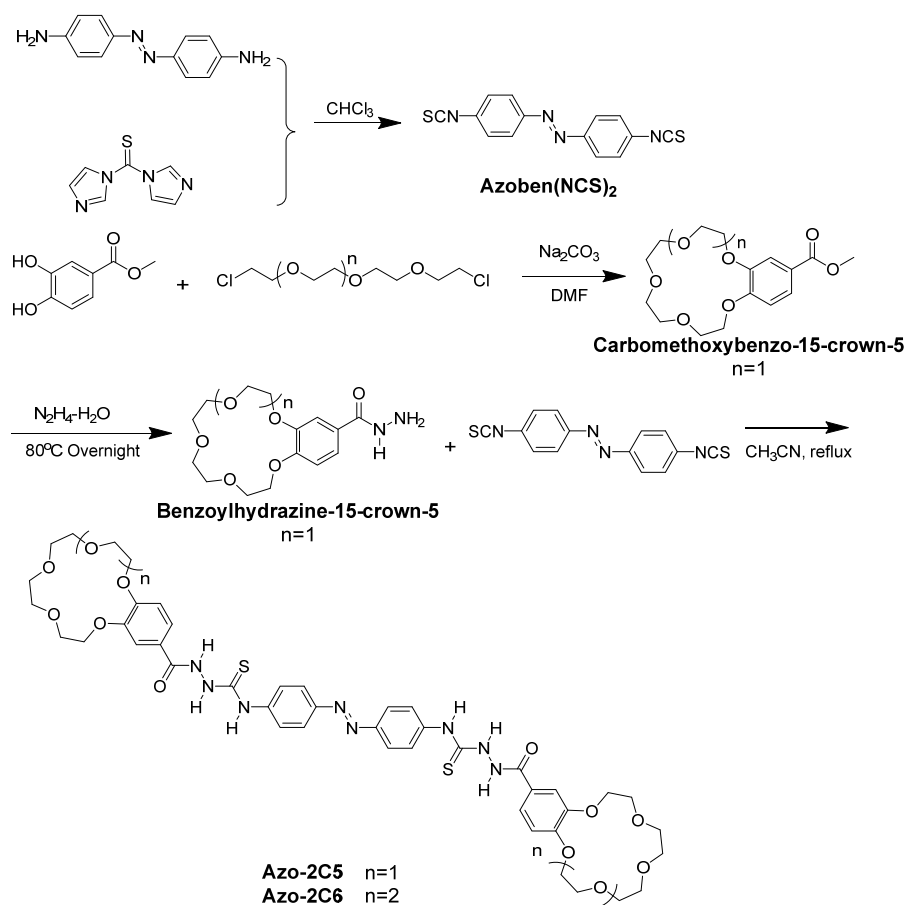
¹ Department of Chemistry, College of Chemistry and Chemical Engineering, The MOE Key Laboratory of Spectrochemical Analysis and Instrumentation, *i*ChEM, Xiamen University, Xiamen 361005, China

² School of Chemistry (F11), The University of Sydney, Sydney, NSW 2006, Australia

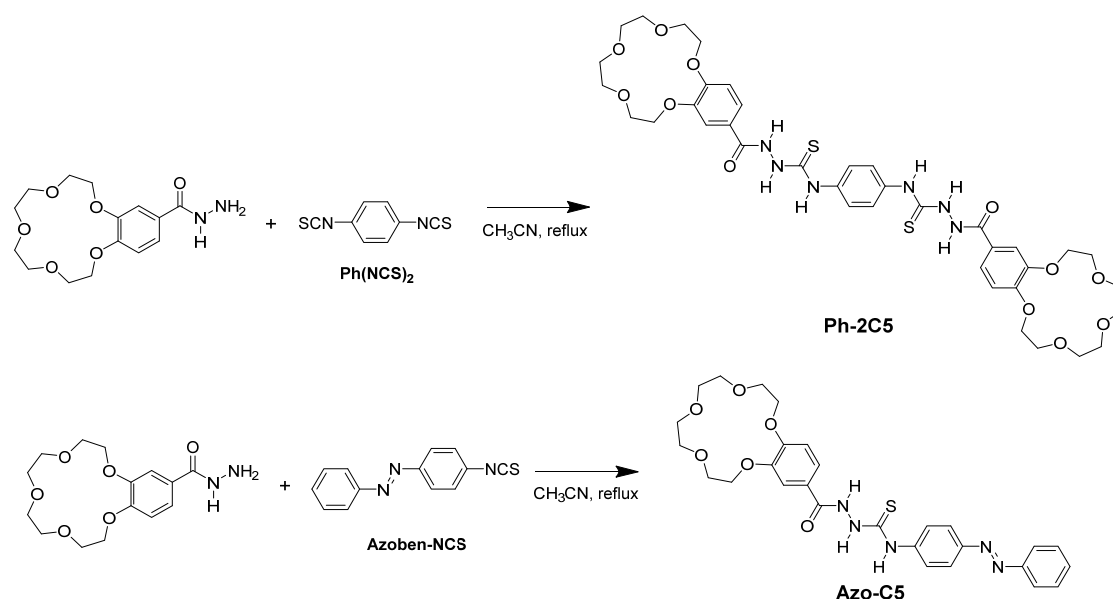
³ The University of Sydney Nano Institute (Sydney Nano), The University of Sydney, Sydney, NSW 2006, Australia

E-mails: xshyan@xmu.edu.cn (Yan X); xin.wu@sydney.edu.au (Wu X); philip.gale@sydney.edu.au (Gale PA); ybjiang@xmu.edu.cn (Jiang Y)

1 Synthetic procedures



Scheme S1 General procedures for the synthesis of **Azo-2C5** and **Azo-2C6**.



Scheme S2 General procedures for the synthesis of **Ph-2C5** and **Azo-C5**.

Azoben(NCS)₂: 4,4'-Azodianiline (10 mmol, 2.12g) was mixed with 1,1'-Thiocarbonyl-diimidazole (25 mmol, 4.46 g) in 50 mL CHCl₃ under vigorous stirring. Using a rotary evaporator to remove the solvent to yield the solid, which was purified by column chromatography with the CHCl₃/MeOH (99:1, v/v) eluent. The solvent was evaporated to give the desired compound as orange solid (2.37 g, 80 % yield).

Carbomethoxybenzo-15-crown-5: The ester was synthesized according to the follow procedure. Methyl 3,4-dihydroxybenzoate (5 g, 29.74 mmol) was add to a DMF (100 mL) solution containing Na₂CO₃ (4 g, 37.74 mmol) under N₂ atmosphere. Then diethylene glycol bis(2-chloroethyl) ether (6.887 g, 29.8 mmol) was add dropwise in 1 h. Refluxing the reaction mixture at 110 °C for 24 h. After cooling the mixture to room temperature, the mixture was filtered and condensed by evaporated *in vacuo*. The obtained viscous oil was further purified by column chromatography with the CHCl₃/MeOH (99:1, v/v) eluent. The solvent was evaporated and recrystallized from ethanol to give the desired compound as white solid (6.41 g, 66 % yield).

Benzoylhydrazine-15-crown-5: Excess amount of hydrazine (85 %, 3.0mL) was added to the **Carbomethoxybenzo-15-crown-5** dissolved in ethanol (50 mL), refluxing the mixture at 80 °C for 12 hours. Evaporating the reaction mixture to get the product, followed by washing with CH₃CN (5 mL) and dired *in vacuo* (2.76 g, 43%).

Azo-2C5: The final product was obtained by refluxing the CH₃CN (50 mL) solution containing **Benzoylhydrazine-15-crown-5** (0.33 g, 1 mmol) and **Azoben(NCS)₂** (0.12 g, 0.4 mmol) at 80°C for 12 hours. The crude product was washed with CH₃CN several times to get pure yellow solid (0.31 g, 82 %).

Azo-2C6: This product was synthesized by the same pathway as **Azo-C5** except replacing the diethylene glycol bis(2-chloroethyl) ether with pentaethylene glycol dichloride.

Ph-2C5: This product was synthesized by refluxing the CH₃CN (50 mL) solution containing **Benzoylhydrazine-15-crown-5** (0.33 g, 1 mmol) and 1,4-phenylene diisothiocyanate (0.08 g, 0.4 mmol) at 80°C for 12 hours. Washing the crude product with CH₃CN to obtain pure white solid (0.20 g, 60 %).

Azo-C5: Equivalent amount of **Benzoylhydrazine-15-crown-5** (0.33 g, 1 mmol) and 4-phenylazophenyl isothiocyanate (0.24 g, 1 mmol) was refluxed in CH₃CN (50 mL) for 12 hours. The product was purified by washing with CH₃CN to afford pure orange solid (0.12 g, 21%).

Azo-2C5: ¹H NMR (500 MHz, DMSO-*d*₆) δ (ppm) 10.42 (s, 2H), 9.96 (s, 2H), 9.86 (s, 2H), 7.85 (d, *J* = 7.8 Hz, 4H), 7.78 (d, *J* = 11.4 Hz, 4H), 7.59 (d, *J* = 7.8 Hz, 2H), 7.55 (s, 2H), 7.06 (d, *J* = 8.5 Hz, 2H), 4.12 (t, *J* = 7.2 Hz, 8H), 3.81 – 3.77 (m, 8H), 3.62 (s, 16H); ¹³C NMR (151 MHz, DMSO-*d*₆) δ(ppm) 181.39, 166.08, 152.17, 149.33, 148.30, 142.65, 126.32, 125.20, 122.70, 122.27, 113.69, 112.81, 70.99, 70.21, 69.23, 68.77; HRMS (ESI): calcd for [C₄₄H₅₈N₈O₁₂S₂Na₂]²⁺/2: 497.1465, found: 497.1481.

Azo-2C6: ¹H NMR (500 MHz, DMSO-*d*₆) δ (ppm) 10.44 (s, 2H), 9.98 (s, 2H), 9.87 (s, 2H), 7.85 (d, *J* = 8.1 Hz, 4H), 7.77 (d, *J* = 8.9 Hz, 4H), 7.58 (d, *J* = 8.5 Hz, 2H), 7.55 (s, 2H), 7.08 (d, *J* = 8.5 Hz, 2H), 4.15 (d, *J* = 2.1 Hz, 8H), 3.78 (t, *J* = 7.8 Hz, 8H), 3.61 (dd, *J* = 4.9, 2.7 Hz, 8H), 3.56 (dd, *J* = 5.4, 3.0 Hz, 8H), 3.53 (s, 8H); ¹³C NMR (151 MHz, DMSO-*d*₆) δ(ppm) 181.30, 166.09, 151.74, 149.23, 147.95, 142.64, 126.30, 125.02, 122.66, 122.03, 112.79, 112.36, 70.40, 70.27, 70.21, 69.08, 68.69; HRMS (ESI): calcd for [C₄₈H₆₀N₆O₁₄S₂Na₂]²⁺/2: 541.1727, found: 541.1743.

Ph-2C5: ¹H NMR (600 MHz, DMSO-*d*₆) δ (ppm) 10.37 (s, 2H), 9.75 (s, 2H), 9.64 (s, 2H), 7.58 (d, *J* = 8.4 Hz, 2H), 7.54 (s, 2H), 7.38 (s, 4H), 7.05 (d, *J* = 8.5 Hz, 2H), 4.14 – 4.10 (m, 8H), 3.81 – 3.77 (m, 8H), 3.62 (s, 16H); ¹³C NMR (214 MHz, DMSO-*d*₆) δ (ppm) 181.50, 166.07, 152.10, 148.24, 136.67, 126.02, 125.29, 122.22, 113.72, 112.77, 70.98, 70.21, 69.22, 68.76; HRMS (ESI): calcd for [C₃₈H₄₈N₆O₁₂S₂Na₂]²⁺/2: 497.1465, found: 497.1481.

Azo-C5: ¹H NMR (850 MHz, DMSO-*d*₆) δ (ppm) 10.44 (s, 1H), 9.99 (s, 1H), 9.90 (s, 1H), 7.89 (s, 4H), 7.80 (s, 2H), 7.60 (s, 3H), 7.56 (s, 2H), 7.07 (s, 1H), 4.13 (s, 4H), 3.80 (s, 4H), 3.63 (s, 8H); ¹³C NMR (214 MHz, DMSO-*d*₆) δ (ppm) 181.32, 166.08, 152.50, 152.18, 149.15, 148.29, 142.94, 131.72, 129.93, 126.31, 125.19, 122.89, 122.22, 118.55, 113.73, 112.81, 70.98, 70.21, 69.23, 68.77; HRMS (ESI): calcd for [C₂₈H₃₁N₅O₆SNa]⁺: 588.1887, found: 588.1894.

2 Ion Transport study and the EC₅₀ measurement

2.1 Cl⁻ transport study

The preparation of LUVs and measurement of transport activity were described in the Experimental. To

quantify the activity of Cl⁻ transport, the salt solution was changed from NaGlc to NMDG-Cl.

2.2 K⁺ transport study

The preparation of LUVs and measurement of transport activity were described in the Experimental. To quantify the activity of K⁺ transport, the salt solution was changed to be KGlc.

2.3 Influence of K⁺ on the transport of Na⁺ and Cl⁻

Preparation of LUVs and transport of Na⁺ and Cl⁻ were conducted by the steps described above. To determine the influence of K⁺, different amounts of KCl solution was added before or during the measurement.

2.4 K⁺ transport (inside to outside) study

The prepared LUVs containing KCl and HPTS inside were transferred to a size exclusion chromatography (stationary phase Sephadex G-50; mobile phase 100 mM NaCl, 10 mM HEPES, pH 7.0) and diluted with the mobile phase to acquire 5 mL lipid stock solution in 2 mM. The obtained stock solution should be used as soon as possible to avoid the ion exchange of Na⁺ and K⁺.

Then we attempt to quantitatively measure the transport activity of K⁺. In each run, 0.1 mL of the lipid stock solution was added to 1.88 mL buffer solution (100 mM NaCl, 10 mM HEPES, pH 7.0) to generate a concentration gradient of K⁺. DMSO (20 μL) solutions of transporters or DMSO (20 μL) was added at the start time. The pH changing inside the LUVs was monitored by HPTS fluorescence ($\lambda_{\text{ex}} = 454 \text{ nm}$, $\lambda_{\text{em}} = 510 \text{ nm}$). At 300 s, 5 μL DMSO solution containing 2 mM FCCP and 10 nM Vln was added to accelerate the uniport process to the end. The fractional fluorescence intensity (I_f) was calculated based on Eq. (1). Different concentrations of carrier molecule were added to obtain a series of fractional fluorescence intensity (I_f). Fitting I_f vs molecule concentration using Eq. (2).

2.5 K⁺ transport (outside to inside) study

Preparation of LUVs and measurement of transport activity were similar to the above experiment, except that the salt solutions inside and outside LUVs were reversed.

2.6 Ion transport mechanism by ²³Na NMR assay

100 mM LUVs stock solution (10 mM HEPES, pH 7.0) with lithium chloride (100 mM) filled inside was prepared based on the way as mentioned above. 5 μL stock solution was added in 400 μL of sodium chloride solution (100 mM NaCl, 10 mM HEPES, pH 7.0) containing 50 μL D₂O. 2 mM DyCl₃ was added to shift extra-vesicular ²³Na peak upfield about 8 ppm to distinguish the signals from intra- and extra-vesicular. After 30 μL DMSO solution was added to the mixture, the ²³Na NMR was utilized to monitor the Na⁺ transport. Then 10 μL of 1 mM **Azo-2C5** was added to start the transport. The ²³Na NMR was taken 10 and 30 minutes later.

2.7 Ion transport mechanism by SPQ assay

The large unilamellar vesicles (LUVs, mean diameter 200 nm) of POPC loaded with chloride-sensitive

fluorescence dye SPQ (0.5 mM) were prepared by freeze/thaw cycles. In each measurement, 0.1 mL of the lipid stock solution was added to 1.88 mL buffer solution (100 mM NMDG-Cl or NaCl, 10 mM HEPES, pH 7.0) to generate a concentration gradient of Cl⁻. DMSO (20 μ L) solutions of transporters or DMSO (20 μ L) was added at the start time. The concentration changing inside the LUVs was monitored by SPQ fluorescence ($\lambda_{\text{ex}} = 360$ nm, $\lambda_{\text{em}} = 430$ nm). At 300 s, Triton X-100 (10 μ L, 20% (v/v)) was added as detergent to lyse the LUVs for calibration. The fractional fluorescence intensity (I_f) was calculated based on Eq. (1).

3 Determination of loading capacity

LUVs (mean diameter 5 μ m) of POPC were prepared by freeze/thaw cycles to acquire 1 mM lipid solution.

The influence of K⁺ on the transport of Na⁺ was explained by changing of loading capacity when K⁺ was present only outside LUVs. To determine the loading capacity, **Azo-2C5** was added to 4.5 mL lipid solution to get mixture containing 4 μ M transporter and 1 mM lipids, then divided the solution into three part (1.5 mL for each one). Centrifuging the first one to separate the lipids and solution (**Fig. S19**), measure the absorption of solution to get the amounts of transporter outside LUVs, then dilute the lipids to 1.5 mL and lyse the lipids to measure the amounts of transporter inside LUVs, *i.e.*, the loading capacity. The second sample was handled the similar way as the first one, but adding KCl (100 mM) to the suspension before centrifugation. The third sample was lysed directly without centrifugation to measure the absorption of the mixture.

The loading capacity was also applied to explain the mechanism of K⁺ transport from inside to outside. POPC LUVs (mean diameter 5 μ m) with KGlc encapsulated was prepared and diluted to acquire 1 mM lipid solution. Part of the lipid solution was transferred to a size exclusion chromatography (stationary phase Sephadex G-50; mobile phase 100 mM NaGlc, 10 mM HEPES, pH 7.0) and diluted with the mobile phase to acquire 5 mL of 1 mM lipid stock solution. Absorption spectra were measured according to the method described above.

4 Ion transport mechanism study

4.1 Ion transport mechanism by calcein leakage assay

POPC LUVs (mean diameter 200 nm) encapsulating calcein (100 mM) were prepared by freeze/thaw cycles. For each measurement, 0.1 mL of the lipid stock solution was added to a 1.88 mL buffer solution to a final lipid concentration of 100 μ M. DMSO (20 μ L) solutions of transporters or DMSO (20 μ L) was added at time 0. The fluorescence emission at time t ($\lambda_{\text{ex}} = 495$ nm, $\lambda_{\text{em}} = 515$ nm) was recorded over 5 min. At 300 s, Triton X-100 (10 μ L, 20% (v/v)) was added as detergent to lyse the

LUVs for calibration. The fractional fluorescence intensity (I_f) was calculated based on Eq. (1).

4.2 Ion transport mechanism study by DPPC experiments

DPPC LUVs (mean diameter 200 nm) were prepared by freeze/thaw cycles as described above (water bath was maintained at 55 °C). The transport of Na⁺, Cl⁻ and K⁺ were performed by the same way as mentioned above. The lipid solution was stirred and thermostated in a polystyrene cuvette at 31 °C, 37 °C or 43 °C.

5 Ions binding study

5.1 Spectral titrations

The Cl⁻ binding affinity with transporters was determined by absorption spectral titrations. The host compounds were dissolved in DMSO to give 1 mM stock solutions. Then diluting the stock solutions in CH₃CN to obtain a final concentration of 20 μM in 5:95 (v/v) DMSO/CH₃CN mixtures. TBA salts were prepared in CH₃CN with a concentration of 1.6 M.

5.2 Isothermal titration calorimetry (ITC) assay

ITC experiments were conducted by TA NANO ITC (25 °C). The host compounds were dissolved in DMSO to give 1 mM stock solutions. Then diluting the stock solutions in CH₃CN to obtain a final concentration of 20 μM in 5:95 (v/v) DMSO/CH₃CN mixtures. Hexafluorophosphate salts were prepared in 5:95 (v/v) DMSO/CH₃CN mixtures with a concentration of 2 mM (NaPF₆) or 1 mM (KPF₆). Consecutive injections of 2 μL hexafluorophosphate salts were dispensed into the host solution at 90 s intervals. The initial injection was discarded in the fitting process when necessary. Solvent consisting of 5:95 (v/v) DMSO/CH₃CN was also prepared as control experiments, which showed no detectable effect of dilution.

6 Supplemental Figures

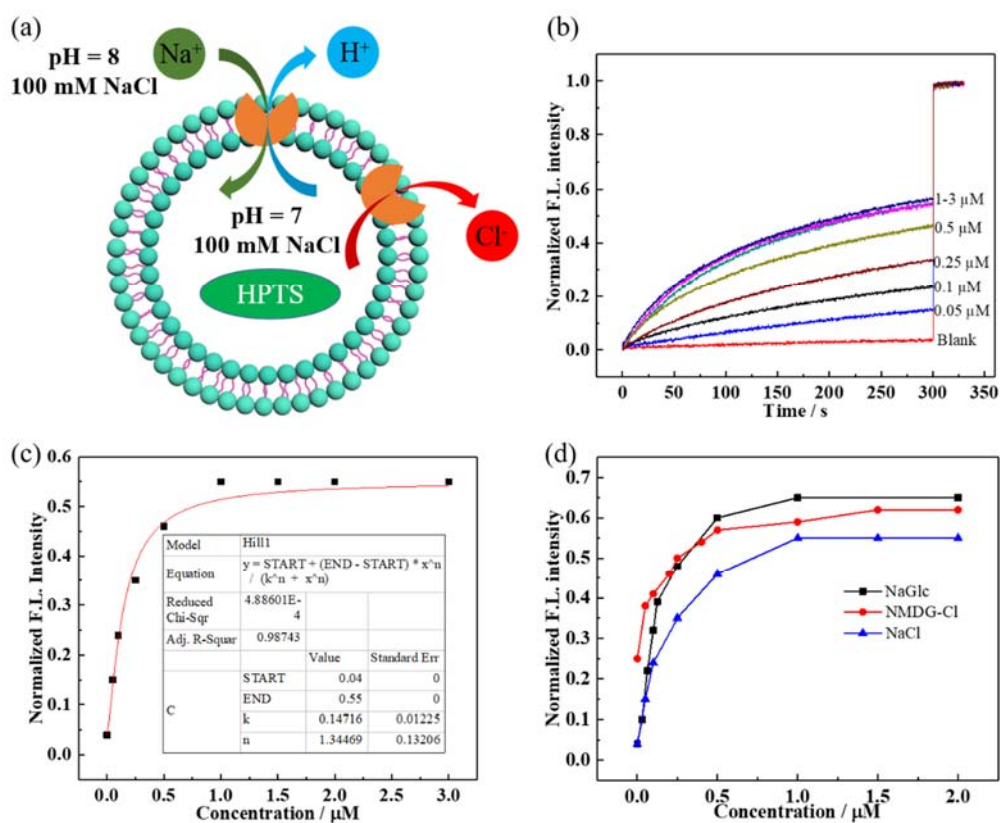


Fig. S1 (a) Schematic representation of quantitative measurement of the ion transport when both Na^+ and Cl^- are present, conducted by applying a pH gradient of 7 inside and 8 outside in LUVs (mean diameter 200 nm) encapsulating pH-sensitive dye HPTS. Inside LUVs: 0.1 mM HPTS, 100 mM NaCl, 10 mM HEPES, pH 7.0. Outside LUVs: 100 mM NaCl, 10 mM HEPES, pH 8.0. (b) Normalized fluorescence intensity obtained by addition of different concentrations of **Azo-2C5** ranging from 0 to 3.0 μM . (c) Hill analysis of ion transport facilitated by **Azo-2C5** when both Na^+ and Cl^- are present. (d) Point data of different transport activities measured in NaGlc (black square), NMDG-Cl (red circle) and NaCl (blue triangle).

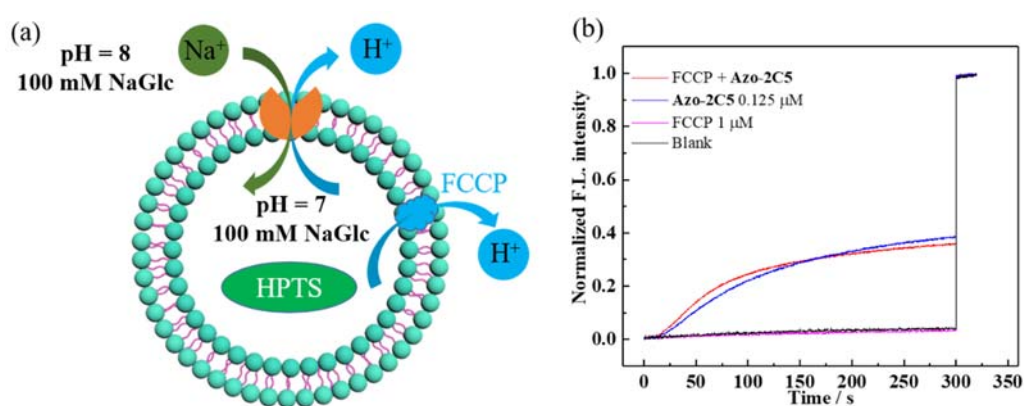


Fig. S2 (a) Schematic representation of the measurement of Na^+ transport coupled with proton transport, conducted by applying a pH gradient of 7 inside and 8 outside in LUVs (mean diameter 200 nm) encapsulating pH-sensitive dye HPTS. Inside LUVs: 0.1 mM HPTS, 100 mM NaGlc, 10 mM HEPES, pH 7.0. Outside LUVs: 100 mM NaGlc, 10 mM HEPES, pH 8.0. (b) Normalized fluorescence intensity obtained by addition of different concentrations of **Azo-2C5** ranging from 0 to 3.0 μM .

transporter FCCP. (b) Na^+ transport activities of **Azo-2C5** ($0.125 \mu\text{M}$) measured in the absence or presence of proton transporter FCCP ($1 \mu\text{M}$).

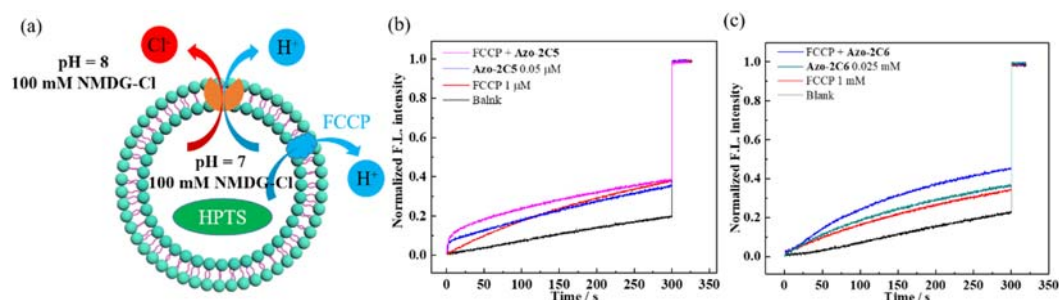


Fig. S3 (a) Schematic representation of quantitative measurement of Cl^- transport coupled with proton transporter FCCP. Cl^- transport activities of **Azo-2C5** ($0.05 \mu\text{M}$, b) and **Azo-2C6** ($0.025 \mu\text{M}$, c) measured in the absence or presence of proton transporter FCCP ($1 \mu\text{M}$).

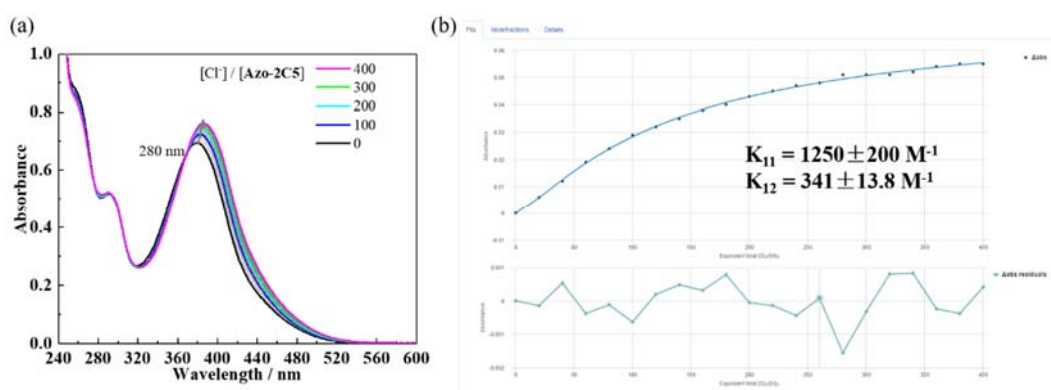


Fig. S4 (a) Absorption spectra of **Azo-2C5** in CH_3CN in the presence of Cl^- . $[\text{Azo-2C5}] = 20 \mu\text{M}$, $[\text{Cl}^-] = 0$ to 8 mM . Cl^- exists as the $(n\text{-Bu})_4\text{N}^+$ salt. (b) Plots of absorbance (380 nm) against the concentration of Cl^- . Fitting results (absorbance at 380 nm , $K_{11} = 1250 \text{ M}^{-1}$, $K_{12} = 341 \text{ M}^{-1}$) calculated using global fitting analysis from [supramolecular.org](http://www.supramolecular.org) (<http://www.supramolecular.org>, accessed Jan 14, 2021). The fitting is based on the 1:2 model.

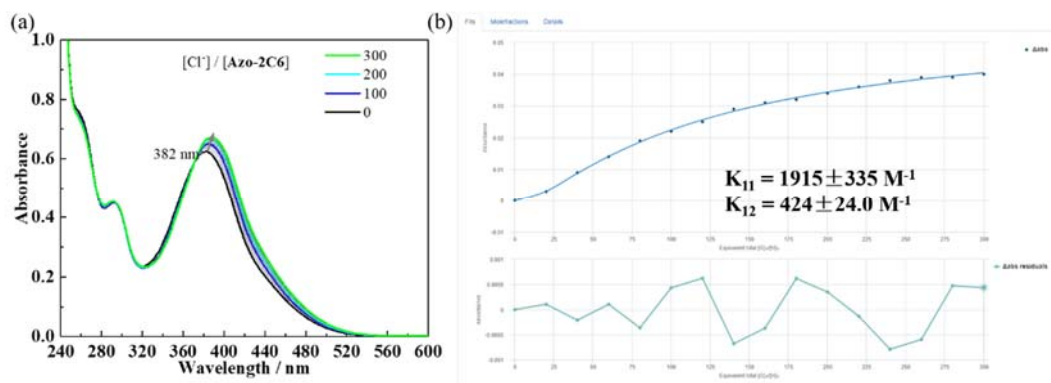


Fig. S5 (a) Absorption spectra of **Azo-2C6** in CH_3CN in the presence of Cl^- . $[\text{Azo-2C6}] = 20 \mu\text{M}$, $[\text{Cl}^-] = 0$ to 6 mM . Cl^- exists as the $(n\text{-Bu})_4\text{N}^+$ salt. (b) Plots of absorbance (382 nm) against the concentration of Cl^- . Fitting results (absorbance at 380 nm , $K_{11} = 1915 \text{ M}^{-1}$, $K_{12} = 424 \text{ M}^{-1}$)

calculated using global fitting analysis from supramolecular.org (<http://www.supramolecular.org>, accessed Jan 14, 2021). The fitting is based on the 1:2 model.

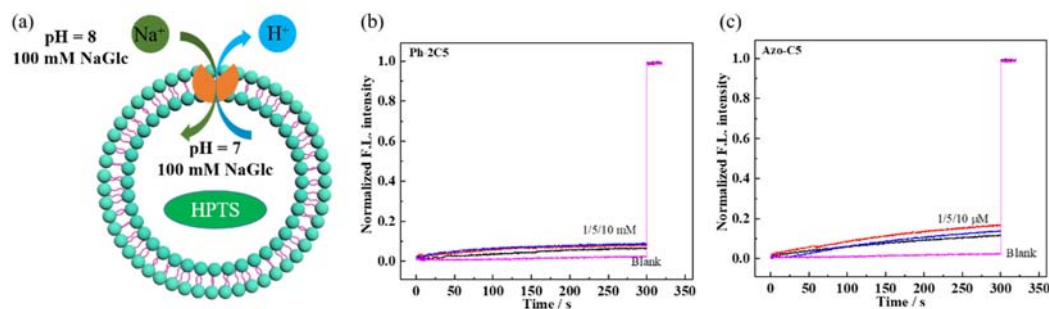


Fig. S6 (a) Schematic representation of quantitative measurement of Na⁺ transport. (b) Normalized fluorescence intensity obtained by addition of different concentrations of **Ph-2C5** (a) and **Azo-C5** (b) ranging from 1 to 10 μM.

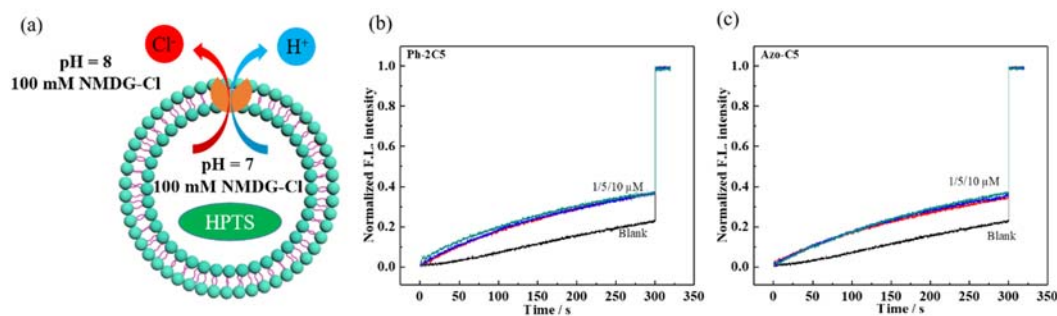


Fig. S7 (a) Schematic representation of quantitative measurement of Cl⁻ transport. Normalized fluorescence intensity obtained by addition of different concentrations of **Ph-2C5** (b) and **Azo-C5** (c) ranging from 1 to 10 μM.

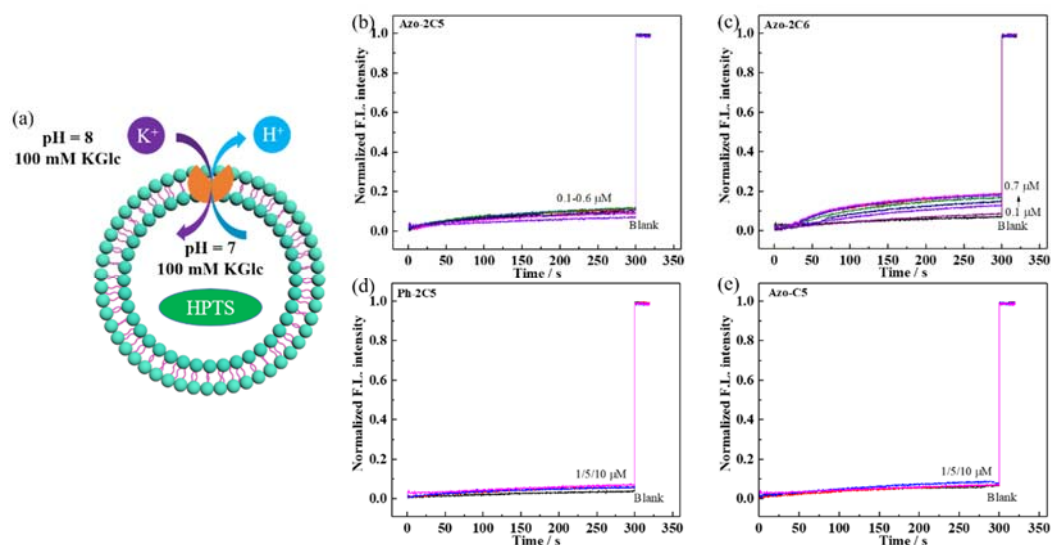


Fig. S8 (a) Schematic representation of quantitative measurement of K^+ transport conducted by applying a pH gradient of 7 inside and 8 outside in LUVs (mean diameter 200 nm) encapsulating pH-sensitive dye HPTS. Inside LUVs: 0.1 mM HPTS, 100 mM KGlc, 10 mM HEPES, pH 7.0. Outside LUVs: 100 mM KGlc, 10 mM HEPES, pH 8.0. Normalized fluorescence intensity obtained by addition of different concentrations of **Azo-2C5** (0 – 0.6 μ M, b), **Azo-C26** (0 – 0.7 μ M, c), **Ph-2C5** (0 – 10 μ M, d) and **Azo-C5** (0 – 10 μ M, e).

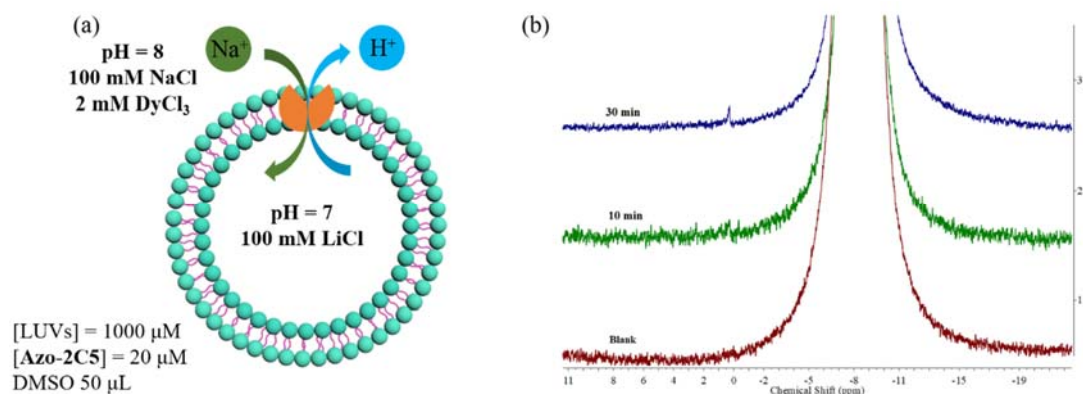


Fig. S9 (a) Schematic representation of qualitative measurement of Na^+ transport conducted by ^{23}Na -NMR. Inside LUVs: 100 mM LiCl, 10 mM HEPES, pH 7.0. Outside LUVs: 100 mM NaCl, 2 mM DyCl₃, 10 mM HEPES, pH 7.0. (b) A series of ^{23}Na -NMR spectra measured after addition of pure DMSO (50 μ L, bottom, incubation for 30 min), **Azo-2C5** (20 μ M, middle, incubation for 10 min) and **Azo-2C5** (20 μ M, top, incubation for 30 min).

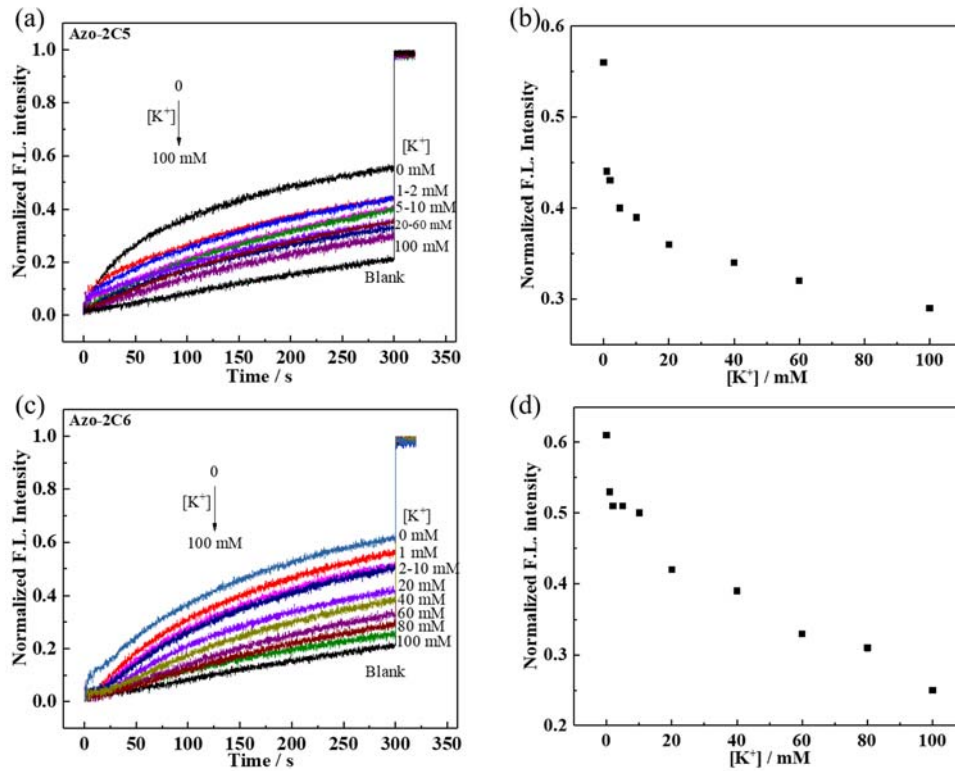


Fig. S10 Normalized fluorescence intensity obtained by addition of **Azo-2C5** (0.5 μM , a) or **Azo-2C6** (0.15 μM , c) and premix of different amounts of KCl. Point data of normalized fluorescence intensity measured by addition of **Azo-2C5** (0.5 μM , b) or **Azo-2C6** (0.15 μM , d) and different concentrations of KCl. Inside LUVs: 0.1 mM HPTS, 100 mM NMDG-Cl, 10 mM HEPES, pH 7.0. Outside LUVs: 100 mM NMDG-Cl, 10 mM HEPES, pH 8.0.

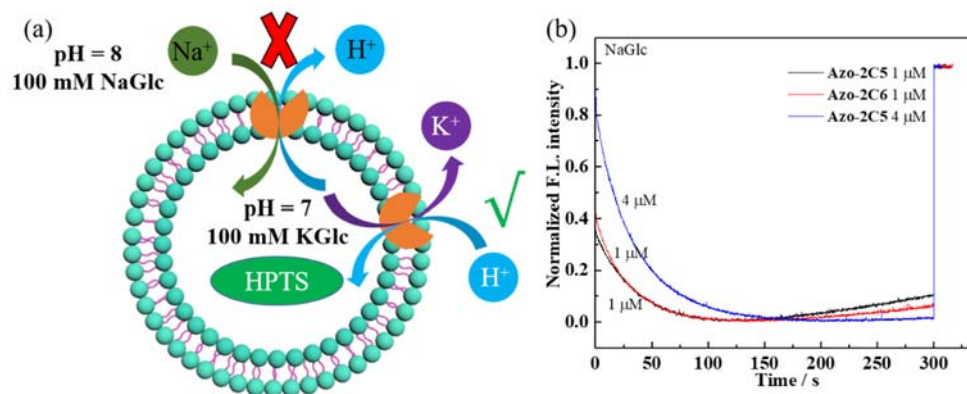


Fig. S11 (a) Schematic representation of qualitative measurement of the ion transport when both pH gradient and concentration gradient of Na^+ were exerted. Inside LUVs: 0.1 mM HPTS, 100 mM KCl, 10 mM HEPES, pH 7.0. Outside LUVs: 100 mM NaCl, 10 mM HEPES, pH 8.0. (b) Normalized fluorescence intensity obtained by addition of different concentrations of **Azo-2C5** (1 μM , black line; 4 μM , blue line) and **Azo-2C6** (1 μM , red line).

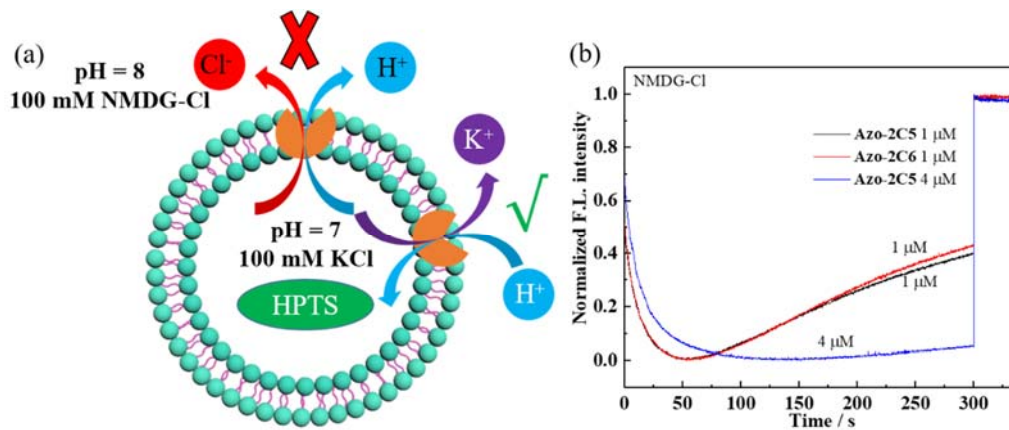


Fig. S12 (a) Schematic representation of qualitative measurement of the ion transport when pH gradient was exerted. Inside LUVs: 0.1 mM HPTS, 100 mM KCl, 10 mM HEPES, pH 7.0. Outside LUVs: 100 mM NMDG-Cl, 10 mM HEPES, pH 8.0. (b) Normalized fluorescence intensity obtained by addition of different concentrations of **Azo-2C5** (1 μ M, black line; 4 μ M, blue line) and **Azo-2C6** (1 μ M, red line).

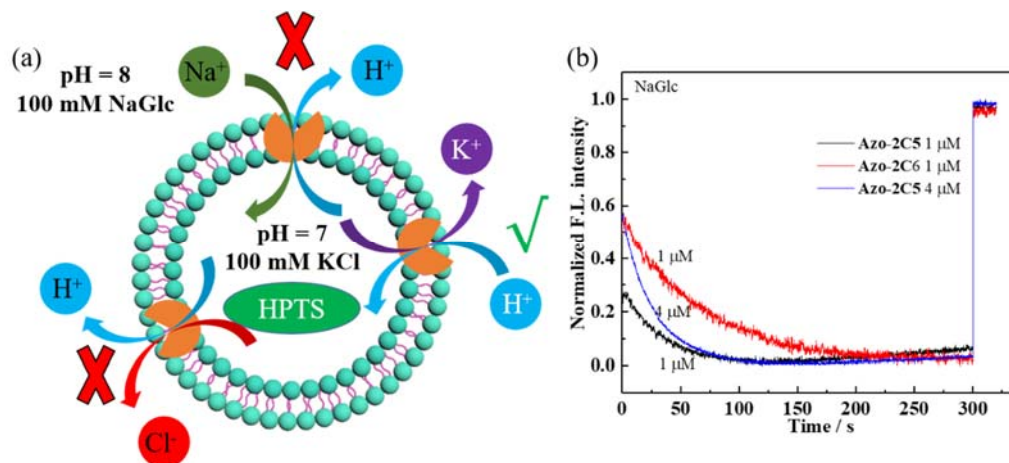


Fig. S13 (a) Schematic representation of qualitative measurement of the ion transport when both pH gradient and concentration gradients of Na^+ and Cl^- were exerted. Inside LUVs: 0.1 mM HPTS, 100 mM KCl, 10 mM HEPES, pH 7.0. Outside LUVs: 100 mM NaGlc, 10 mM HEPES, pH 8.0. (b) Normalized fluorescence intensity obtained by addition of different concentrations of **Azo-2C5** (1 μ M, black line; 4 μ M, blue line) and **Azo-2C6** (1 μ M, red line).

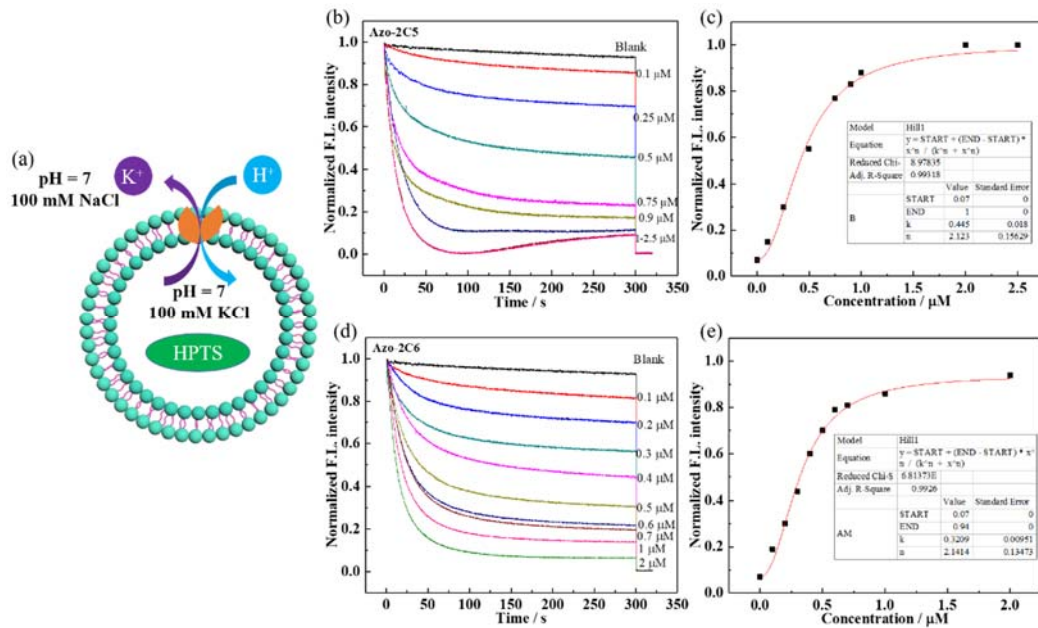


Fig. S14 (a) Schematic representation of quantitative measurement of K⁺ transport (from inside to outside) conducted by exerting concentration gradient of K⁺ in LUVs (mean diameter 200 nm) encapsulating pH-sensitive dye HPTS. Inside LUVs: 0.1 mM HPTS, 100 mM KGlc, 10 mM HEPES, pH 7.0. Outside LUVs: 100 mM NaGlc, 10 mM HEPES, pH 7.0. Normalized fluorescence intensity obtained by addition of different concentrations of **Azo-2C5** (0 – 3.0 μM, b) or **Azo-2C6** (0 – 2.0 μM, d). Hill analysis of K⁺ uniport facilitated by **Azo-2C5** (c) or **Azo-2C6** (e).

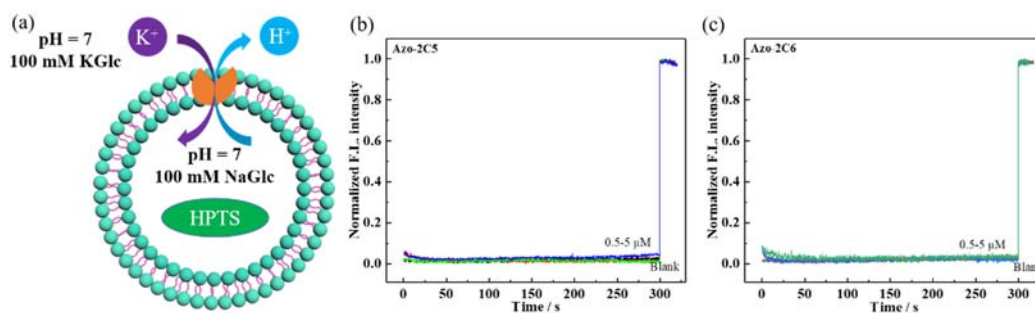


Fig. S15 (a) Schematic representation of quantitative measurement of K⁺ transport conducted by exerting concentration gradient of K⁺ in LUVs (mean diameter 200 nm) encapsulating pH-sensitive dye HPTS. Inside LUVs: 100 mM NaGlc, 10 mM HEPES, pH 7.0. Outside LUVs: 100 mM KGlc, 10 mM HEPES, pH 7.0. Normalized fluorescence intensity obtained by addition of different concentrations of **Azo-2C5** (b) or **Azo-2C6** (c) ranging from 0 to 5.0 μM.

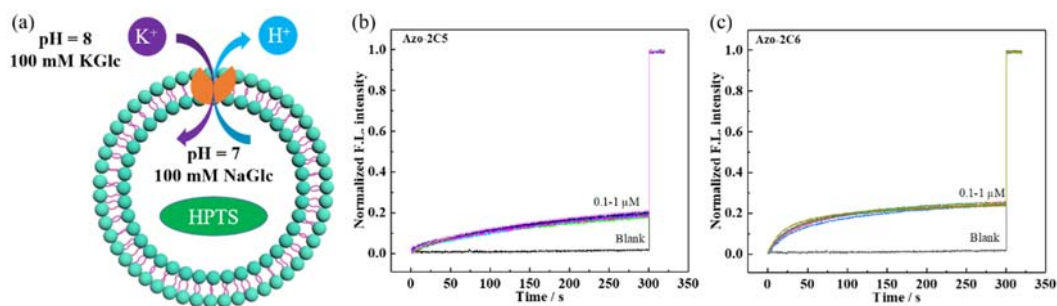


Fig. S16 (a) Schematic representation of quantitative measurement of K^+ transport conducted by exerting both pH gradient and concentration gradient of K^+ in LUVs (mean diameter 200 nm) encapsulating pH-sensitive dye HPTS. Inside LUVs: 0.1 mM HPTS, 100 mM NaGlc, 10 mM HEPES, pH 7.0. Outside LUVs: 100 mM KGlc, 10 mM HEPES, pH 8.0. Normalized fluorescence intensity obtained by addition of different concentrations of **Azo-2C5** (b) or **Azo-2C6** (c) ranging from 0 to 1.0 μ M.

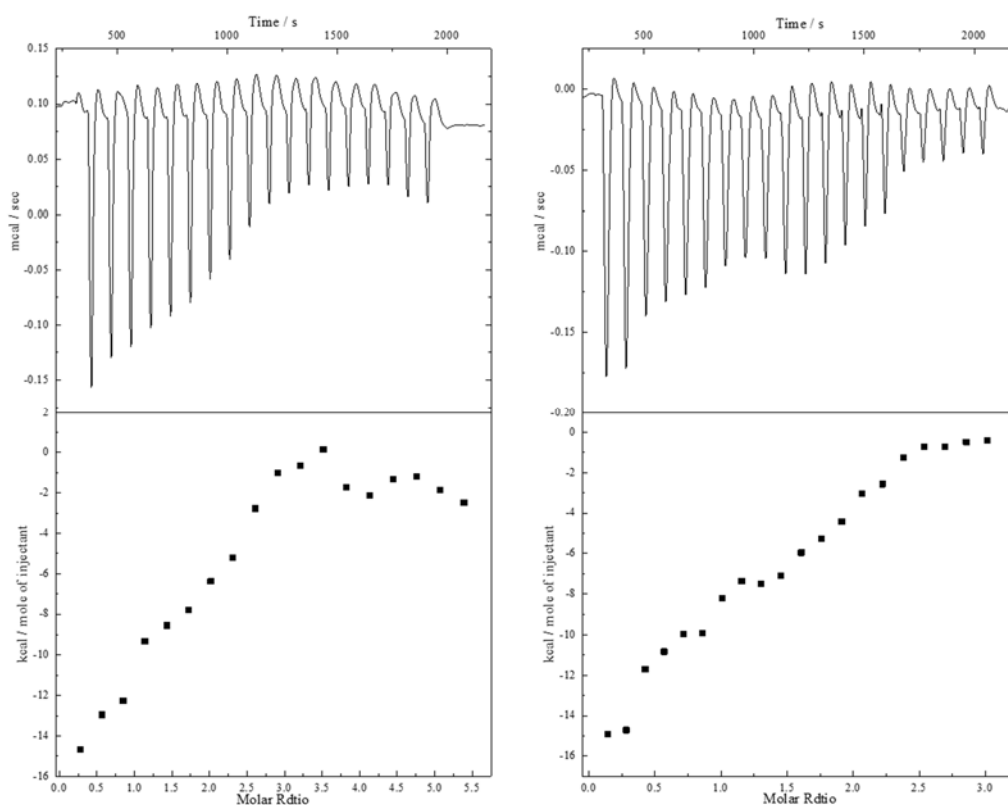


Fig. S17 ITC titrations of **Azo-2C5** in the presence of sodium hexafluorophosphate (left) and potassium hexafluorophosphate (right).

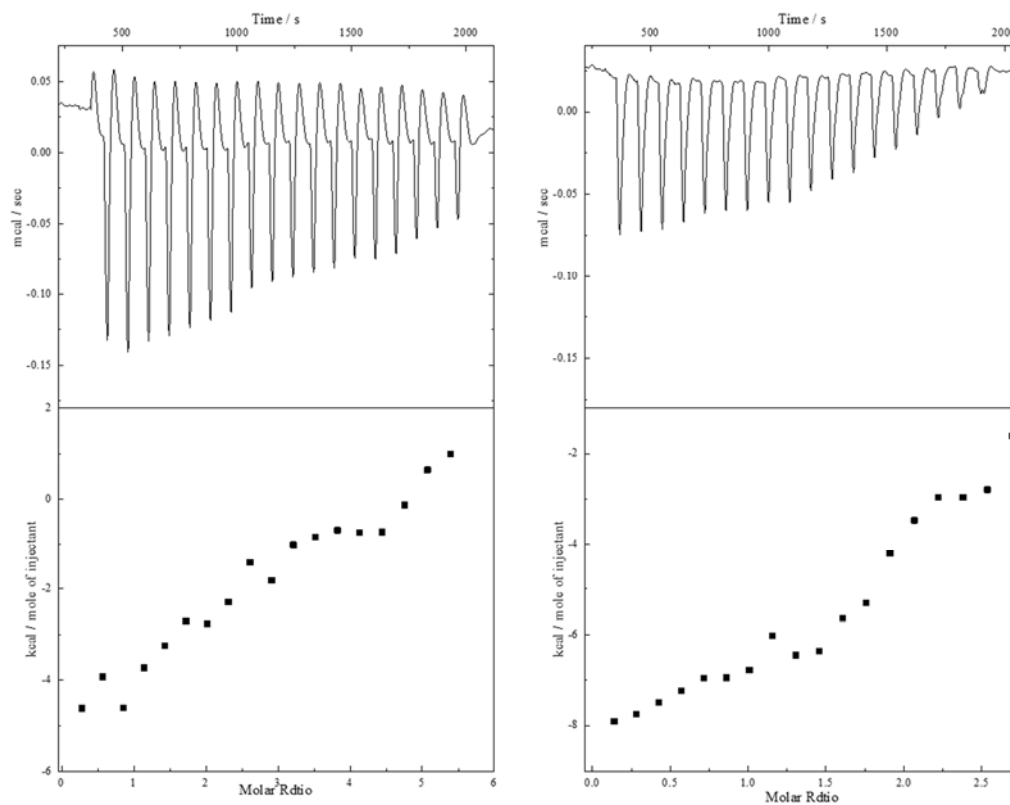


Fig. S18 ITC titrations of Azo-2C6 in the presence of sodium hexafluorophosphate (left) and potassium hexafluorophosphate (right).

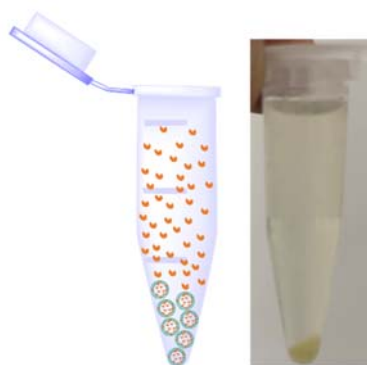


Fig. S19 Assumed distribution of transporters and LUVs after centrifugation (left) and photo taken after centrifugation (right), showing that the LUVs can be well separated by centrifugation.

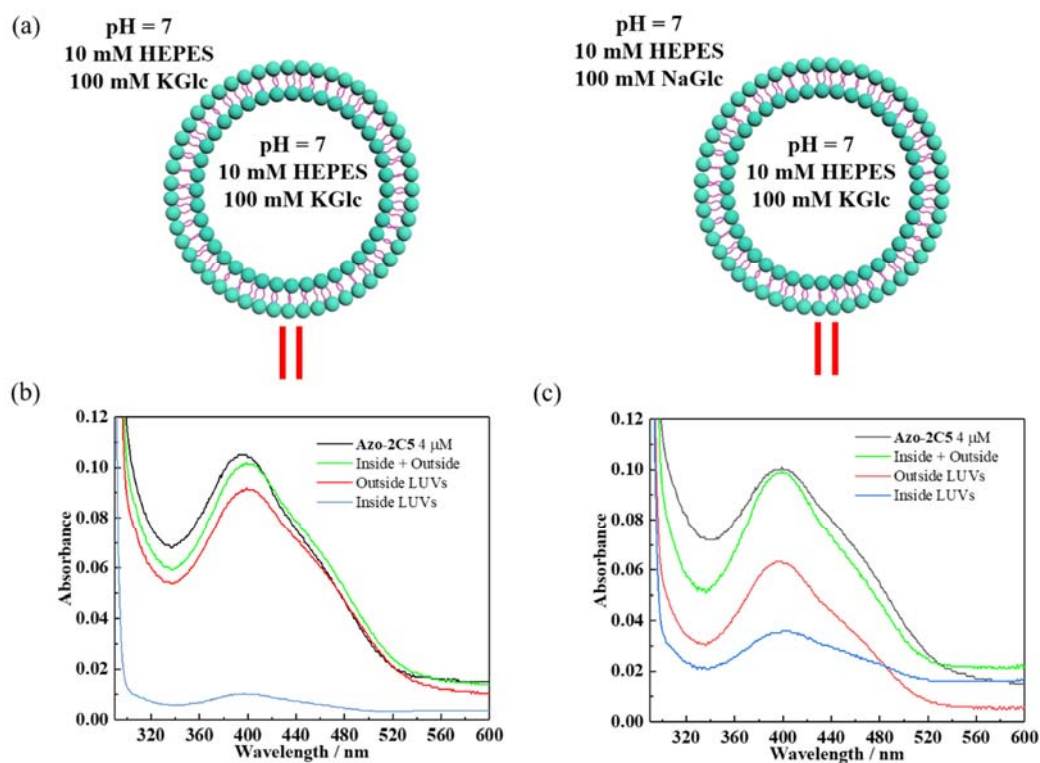


Fig. S20 (a) Schematic representation of test conditions of the absorption spectra. (b, c) Absorption spectra of **Azo-2C5** (4 μM) in lipid suspension (black line) and distributed inside (blue line) and outside (red line) LUVs. Absorption values of inside (blue line) and outside (red line) are added and plotted (green line) to compare with the unseparated one (black line). (b) Inside LUVs: 100 mM KGlc, 10 mM HEPES, pH 7.0. Outside LUVs: 100 mM KGlc, 10 mM HEPES, pH 7.0. (c) Inside LUVs: 100 mM KGlc, 10 mM HEPES, pH 7.0. Outside LUVs: 100 mM NaGlc, 10 mM HEPES, pH 7.0.

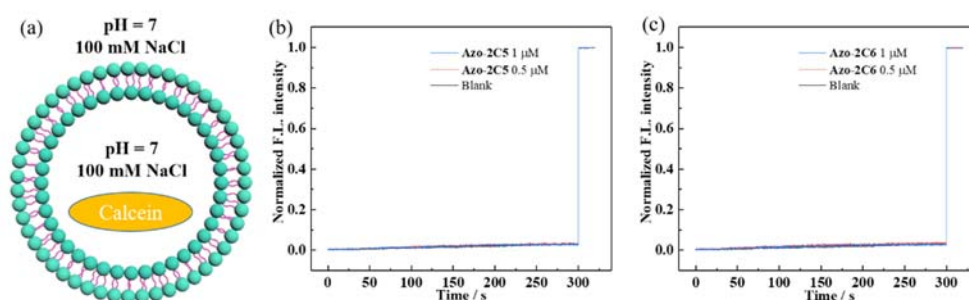


Fig. S21 (a) Schematic representation of calcein leakage assay in the presence of transporters. Normalized fluorescence intensity obtained by addition of different concentrations of **Azo-2C5** (b) and **Azo-2C6** (c) ranging from 0 to 1.0 μM .

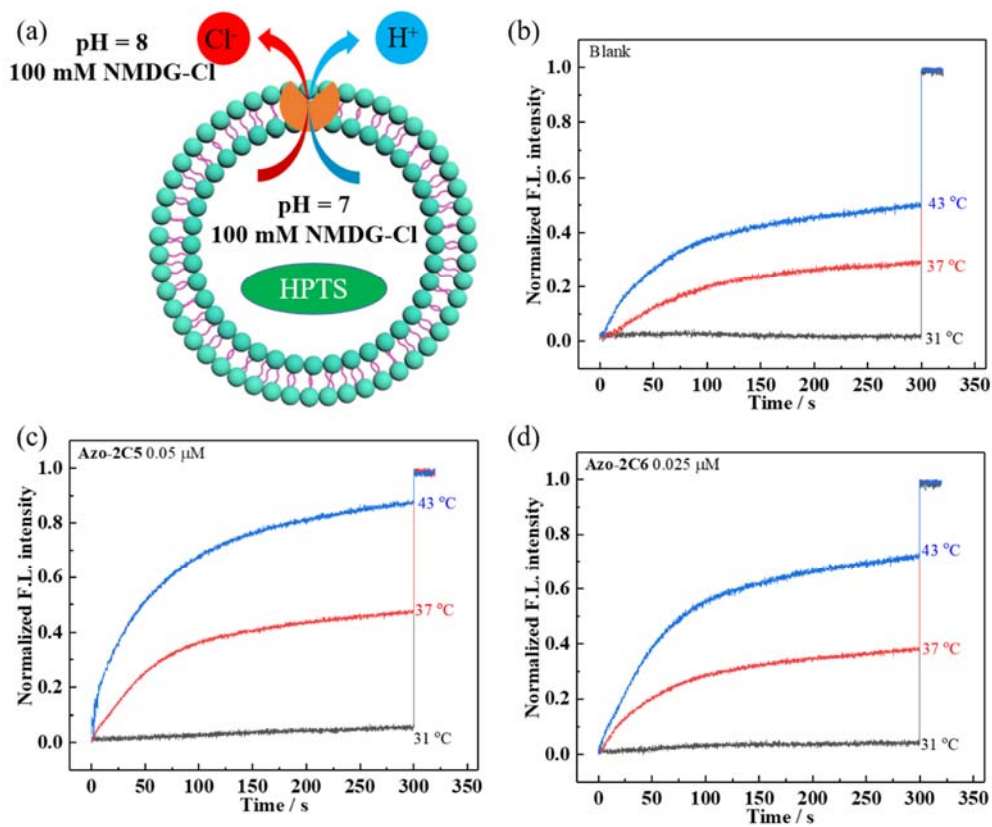


Fig. S22 (a) Schematic representation of DPPC experiments to verify the transport mechanism. Normalized fluorescence intensity obtained by addition of DMSO (20 μ L, b), DMSO solutions of **Azo-2C5** (0.05 μ M, c) and **Azo-2C6** (0.025 μ M, d) at different temperatures ranging from 31 to 43 $^{\circ}$ C.

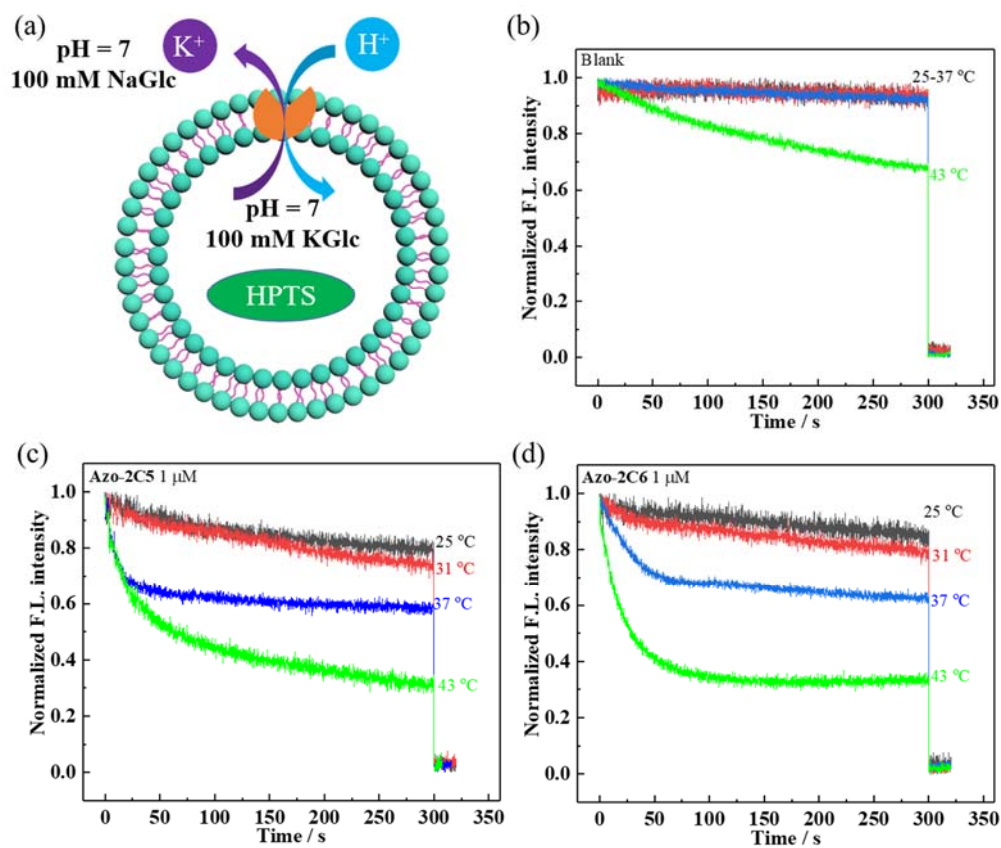


Fig. S23 (a) Schematic representation of DPPC experiments to verify the transport mechanism. Normalized fluorescence intensity obtained by addition of DMSO (20 μL, b), DMSO solutions of **Azo-2C5** (1 μM, c) and **Azo-2C6** (1 μM, d) at different temperatures ranging from 25 to 43 °C.

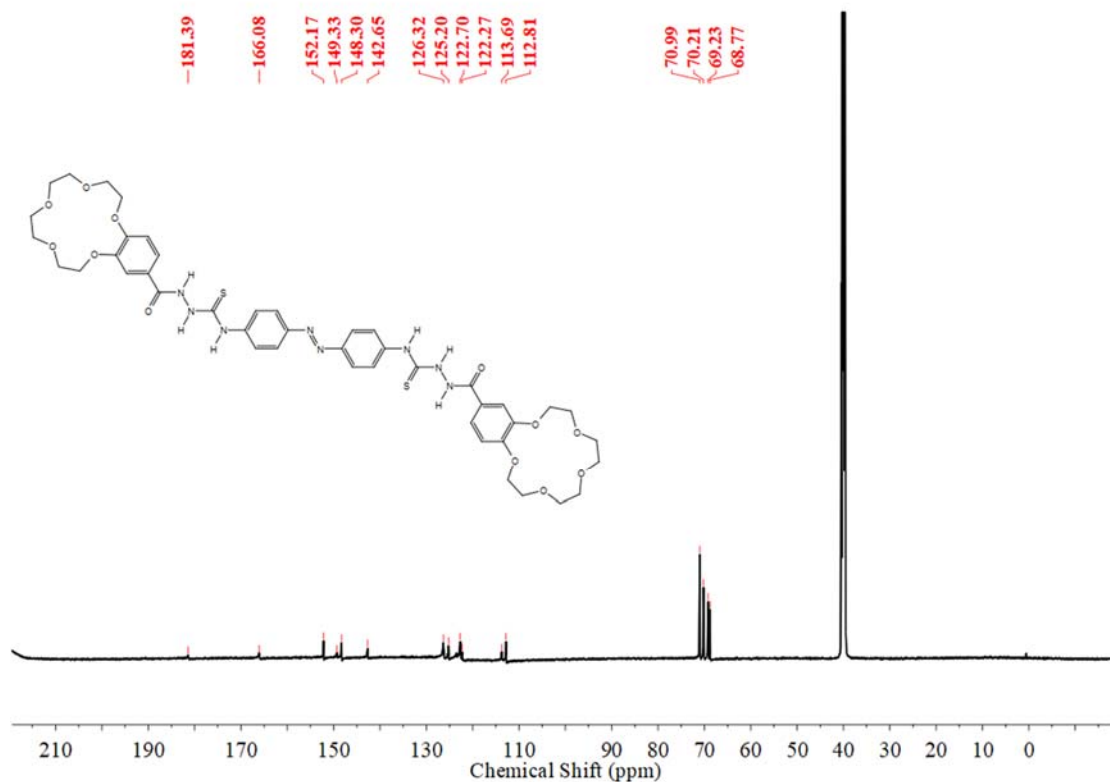
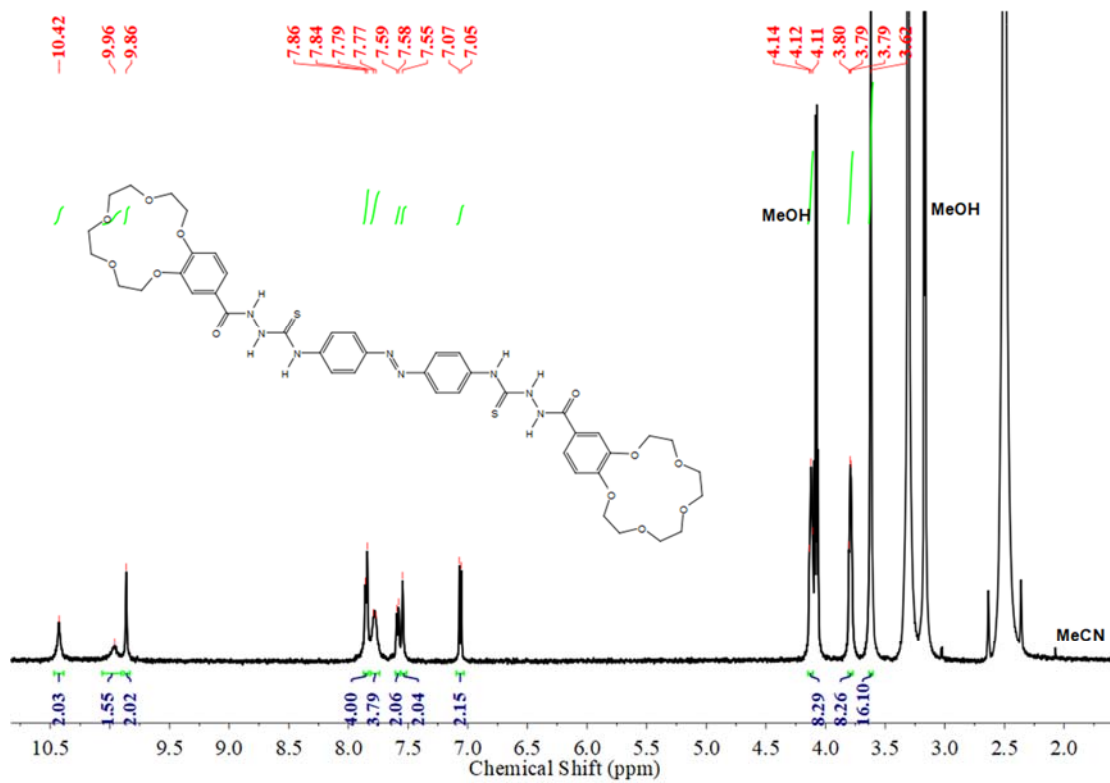


Fig. S24 ¹H and ¹³C NMR spectra of Azo-2C5.

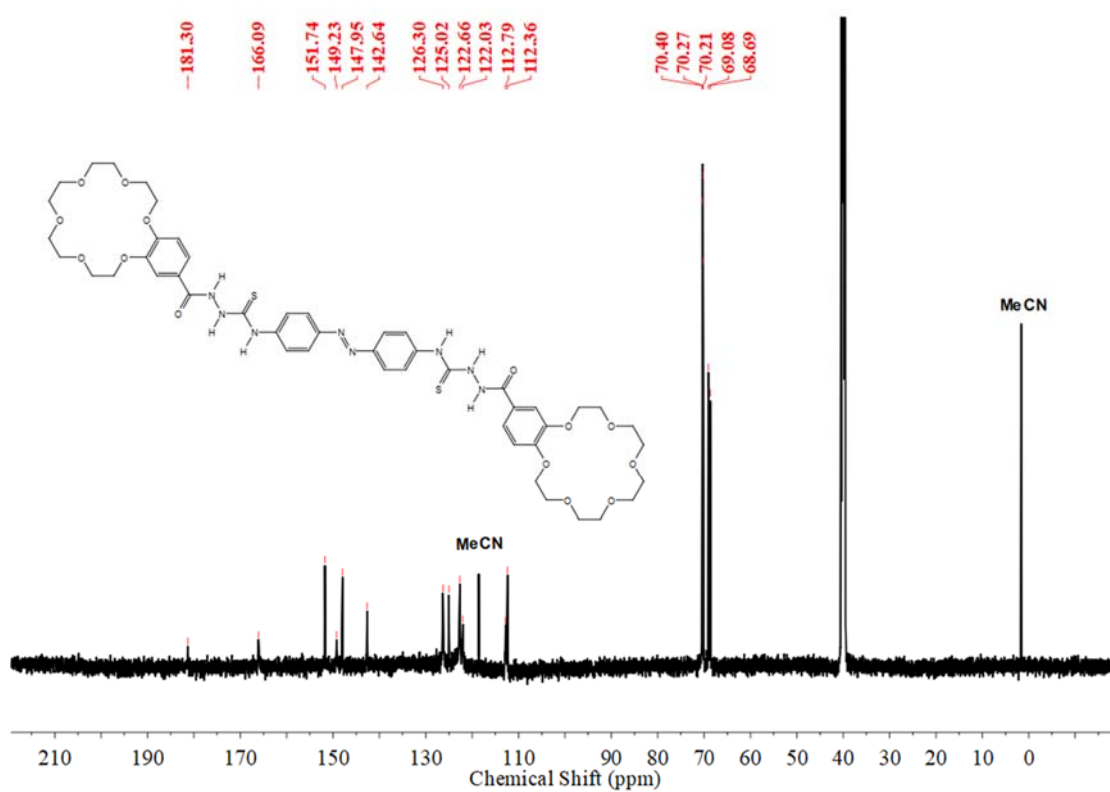
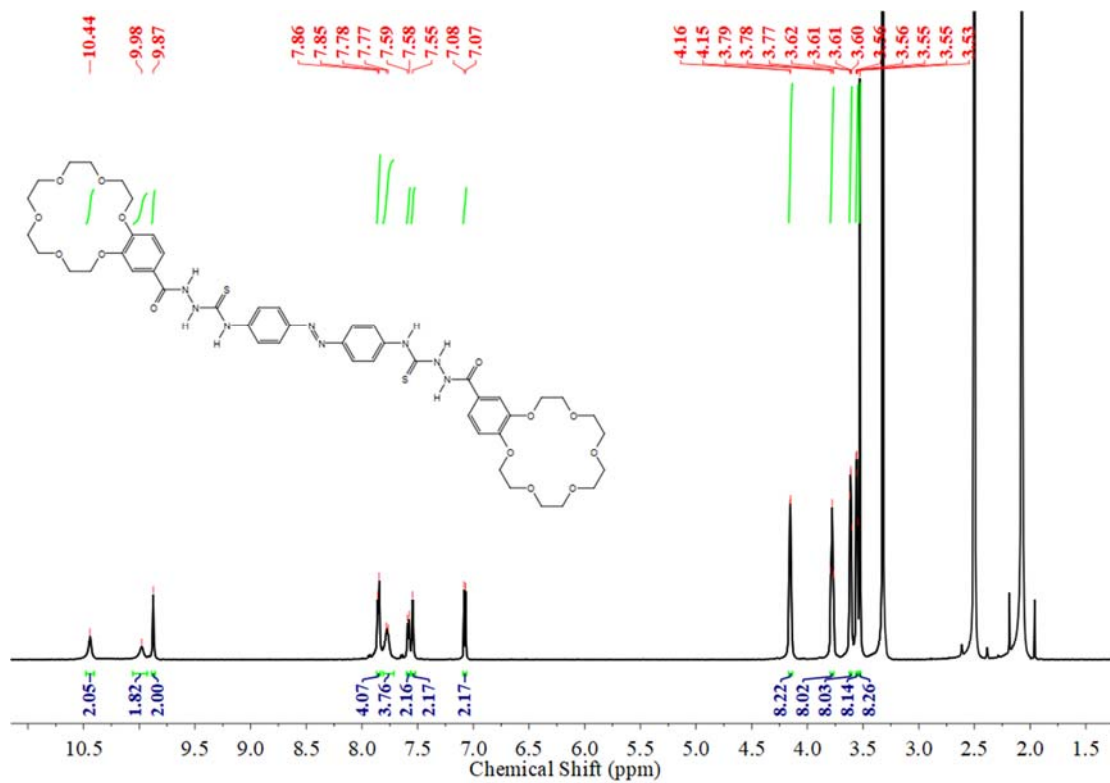


Fig. S25 ^1H and ^{13}C NMR spectra of Azo-2C6.

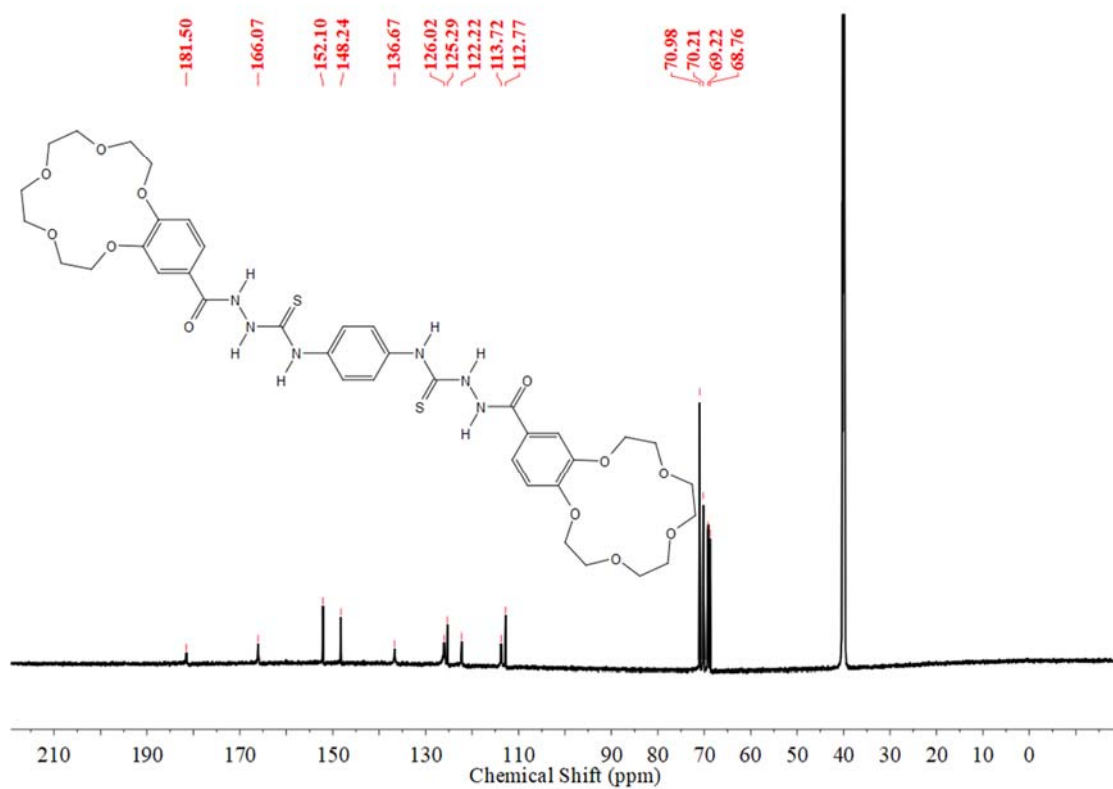
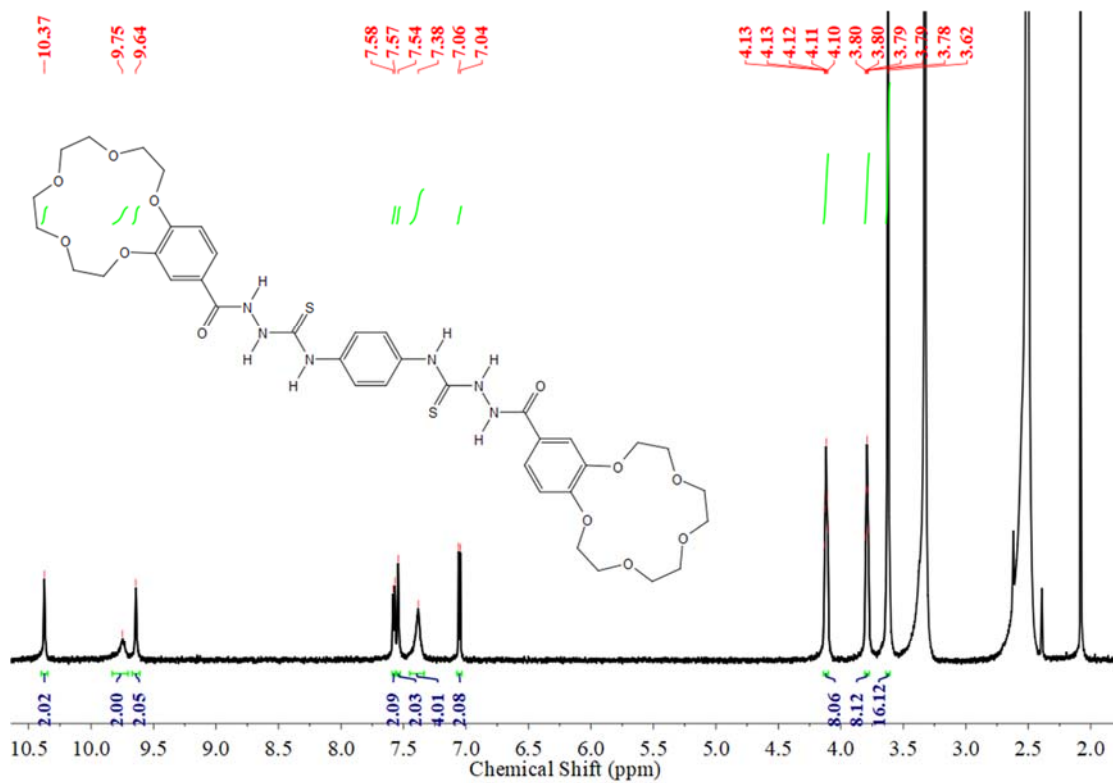


Fig. S26 ¹H and ¹³C NMR spectra of Ph-2C5.

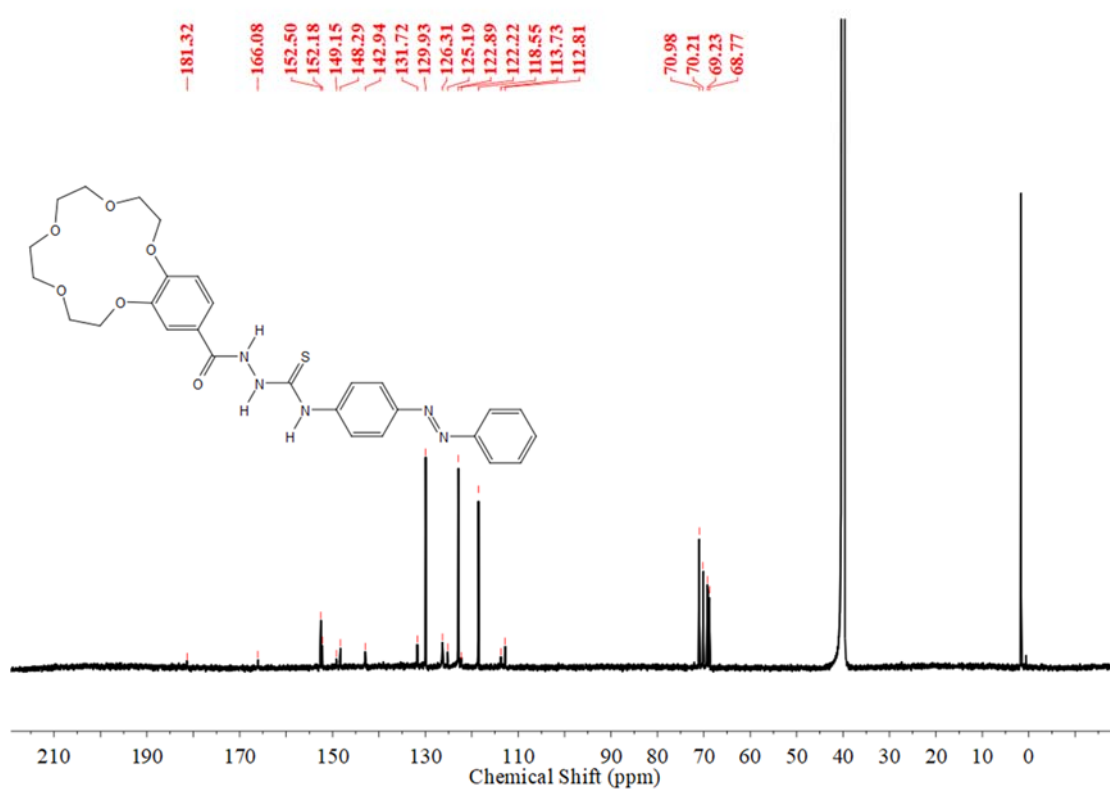
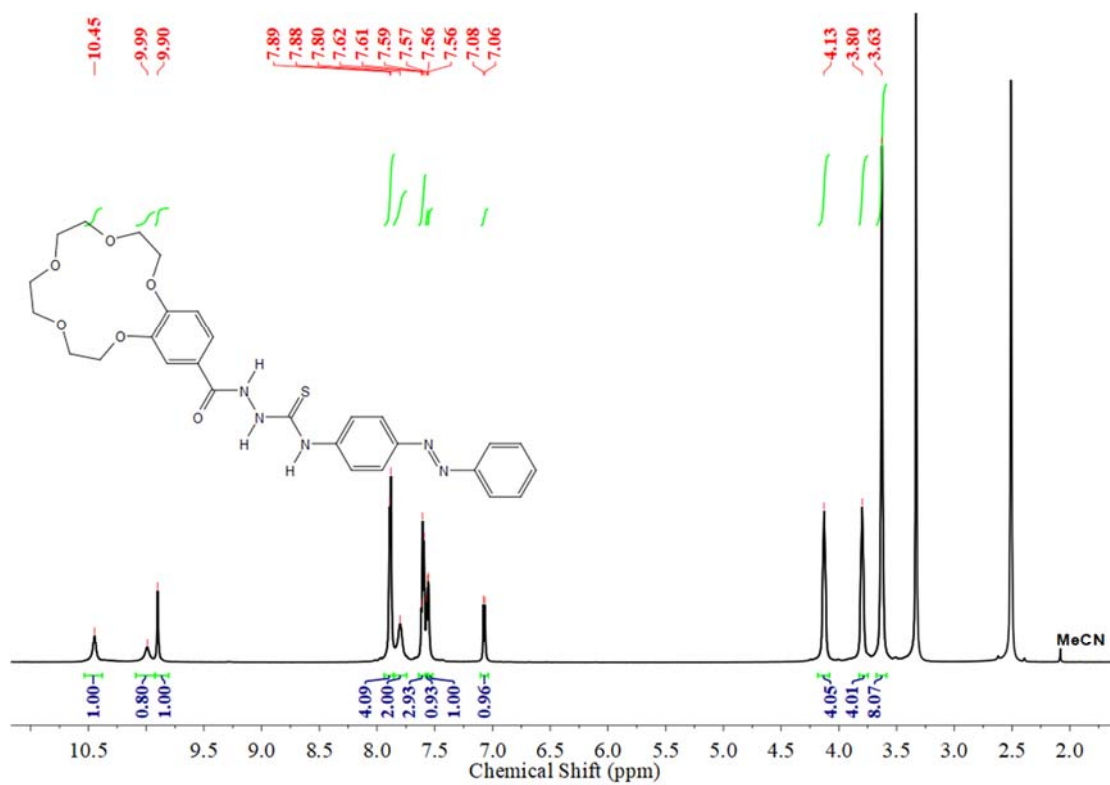


Fig. S27 ^1H and ^{13}C NMR spectra of Azo-C5.

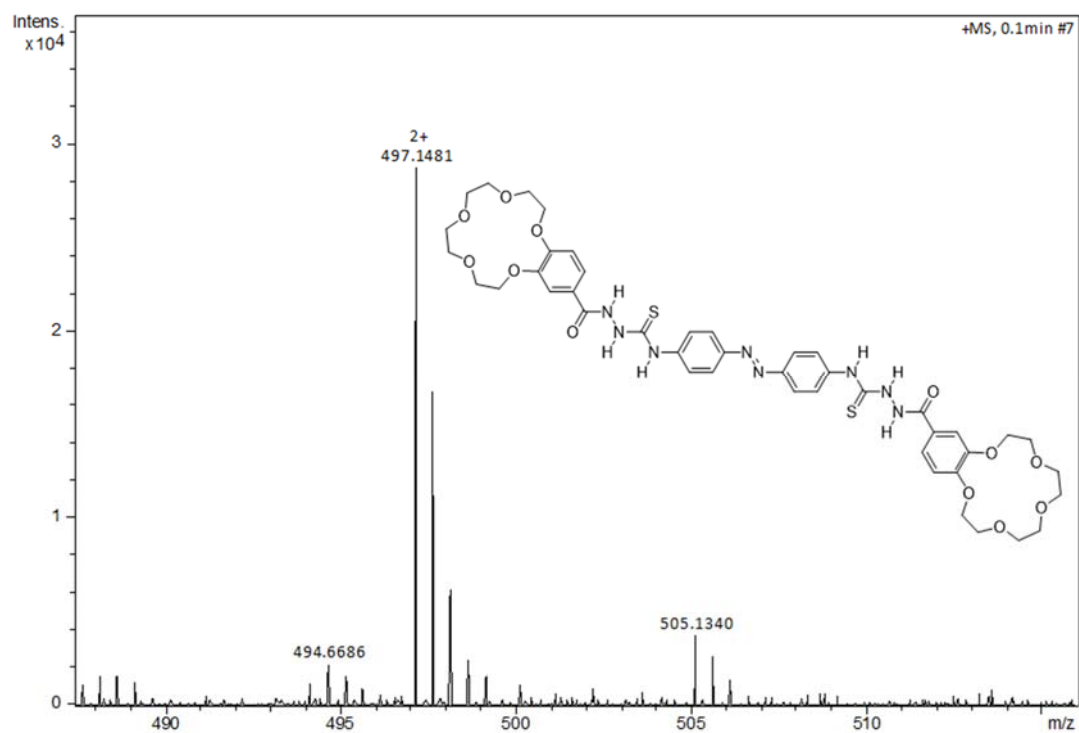


Fig. S28 HRMS (ESI-MS) of Azo-2C5.

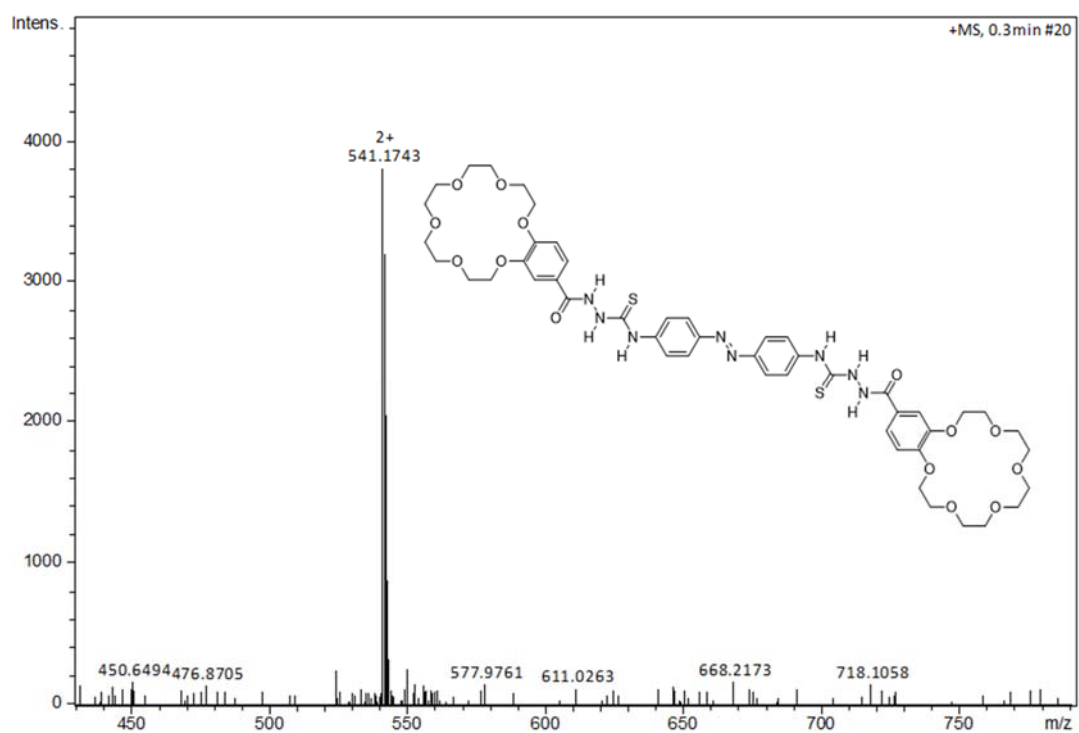


Fig. S29 HRMS (ESI-MS) of Azo-2C6.

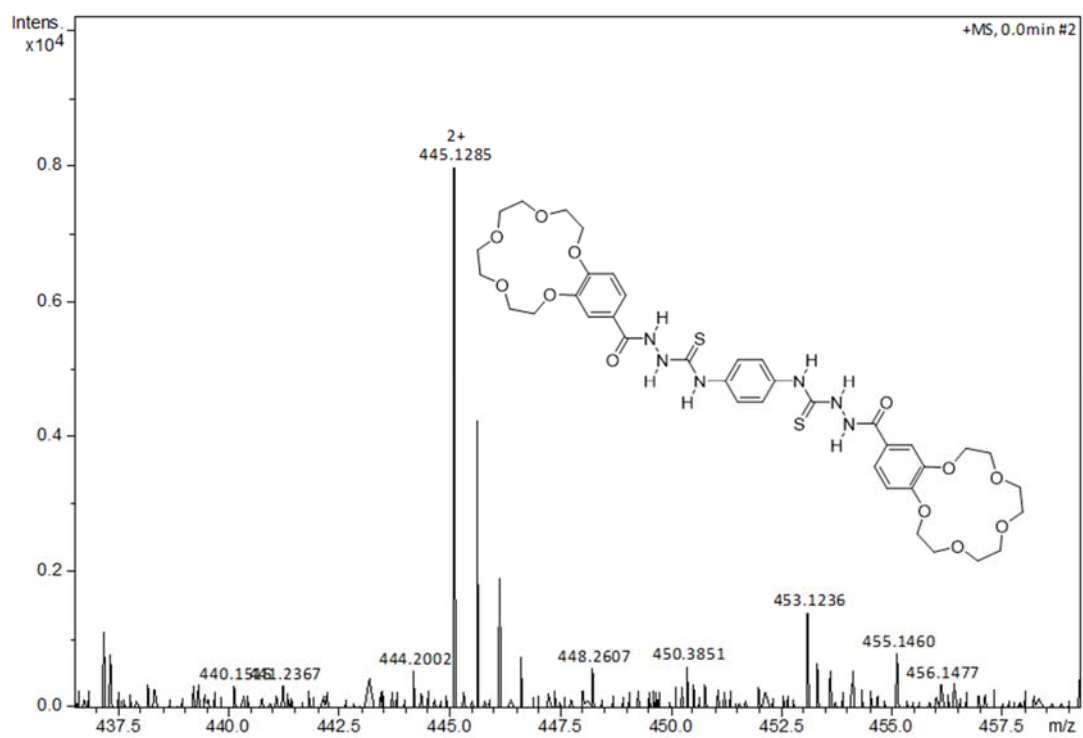


Fig. S30 HRMS (ESI-MS) of Ph-2C5.

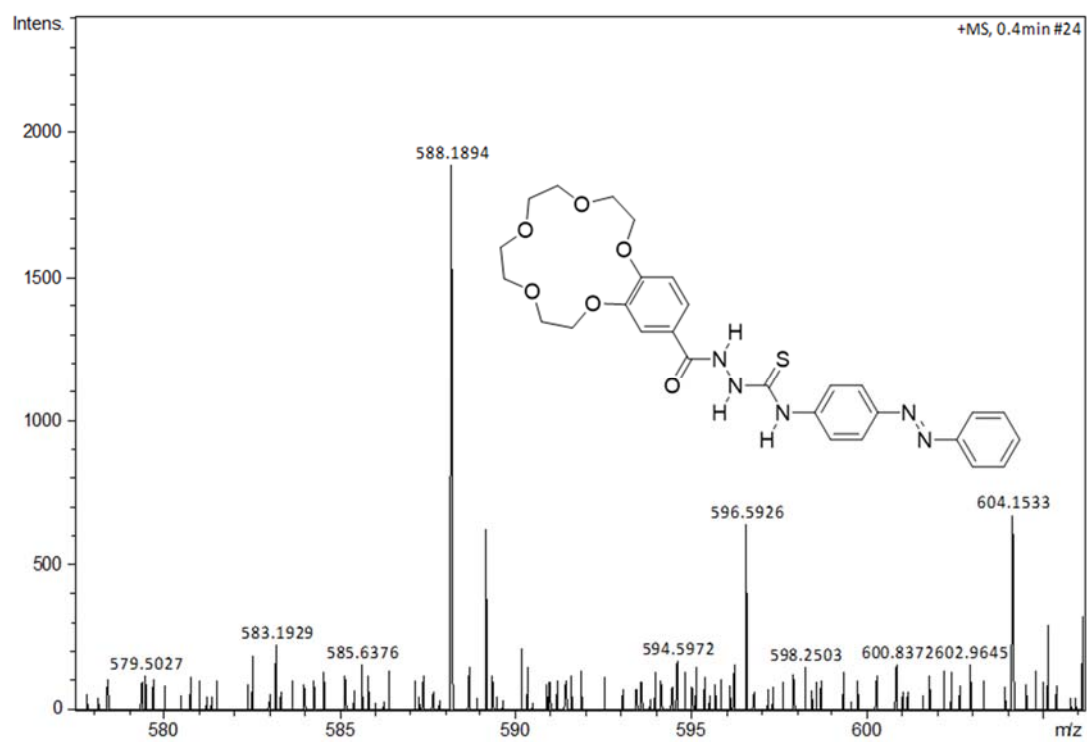


Fig. S31 HRMS (ESI-MS) of Azo-C5.